

UC San Diego

UC San Diego Previously Published Works

Title

Signaling Microdomains in the Spotlight: Visualizing Compartmentalized Signaling Using Genetically Encoded Fluorescent Biosensors.

Permalink

<https://escholarship.org/uc/item/3wg5w7pc>

Authors

Zhang, Jin-Fan
Mehta, Sohum
Zhang, Jin

Publication Date

2021-01-06

DOI

10.1146/annurev-pharmtox-010617-053137

Peer reviewed



Published in final edited form as:

Annu Rev Pharmacol Toxicol. 2021 January 06; 61: 587–608. doi:10.1146/annurev-pharmtox-010617-053137.

Signaling Microdomains in the Spotlight – Visualizing Compartmentalized Signaling Using Genetically Encoded Fluorescent Biosensors

Jin-fan Zhang^{1,2,4}, Sohum Mehta^{1,4}, Jin Zhang^{1,2,3,*}

¹Department of Pharmacology, University of California, San Diego, La Jolla, CA 92093.

²Department of Bioengineering, University of California, San Diego, La Jolla, CA 92093

³Department of Chemistry and Biochemistry, University of California, San Diego, La Jolla, CA 92093

⁴These authors contributed equally.

Abstract

How cells muster a network of interlinking signaling pathways to faithfully convert diverse external cues into specific functional outcomes remains a central question in biology. Through their ability to convert dynamic biochemical activities into rapid and precise optical readouts, genetically encoded fluorescent biosensors have become instrumental in unraveling the molecular logic controlling the specificity of intracellular signaling. In this review, we discuss how the use of genetically encoded fluorescent biosensors to visualize dynamic signaling events within their native cellular context is shedding light on the different strategies employed by cells to organize signaling activities into discrete compartments, or signaling microdomains, to ensure functional specificity.

Keywords

Signal transduction; live-cell imaging; FRET; spatiotemporal dynamics

Introduction

Signaling pathways form the communications and information-processing network through which cells dynamically sense and respond to their changing environment. This network utilizes the often transient biochemical changes and interactions among a diverse yet finite complement of signaling molecules, including cell surface receptors, second messengers, and enzymatic effectors, to decipher various stimuli and encode the flow of information within the intracellular space. Considering the substantial number of components and the multitude of signaling events occurring in parallel in cells, signaling pathways must be carefully coordinated in both space and time to achieve faithful and specific functional

*Correspondence: Jin Zhang, 9500 Gilman Drive, BRF-II 1120, La Jolla, CA 92093-0702, phone (858) 249-0602, jzhang32@ucsd.edu.

outcomes (1). Indeed, the spatial organization, or compartmentation, of the intracellular signaling machinery was first proposed over 40 years ago to explain how specific stimuli can elicit distinct responses despite engaging the same pathway (2, 3). Rather than being homogeneously dispersed throughout the intracellular space, signaling molecules can instead be differentially recruited to, as well as produced or activated within, discrete subcellular locations. Close proximity and dynamic assembly promote efficient functional interactions among the participating signaling molecules while also enabling flexible regulation of their signaling strengths/period. This uneven distribution leads to the formation of various “signaling microdomains” that can enhance signaling specificity to achieve biological diversity within cells and organisms.

Although spatially organized signaling is not an entirely new concept, signaling microdomains have historically been challenging to study due to their highly dynamic nature and tight dependence on the cell’s native molecular environment, which are difficult to capture or recapitulate *in vitro* using traditional biochemical approaches. In contrast, genetically encoded optical tools such as fluorescent protein (FP)-based biosensors can be nondestructively introduced into living cells, thereby maintaining the native cellular context, and with the nanosecond timescales and submicron spatial resolution enabling direct, real-time visualization of dynamic signaling events *in situ* with high spatial and temporal precision. More detailed spatial information can also be obtained by co-opting the cell’s intrinsic protein expression machinery to send biosensors to specific subcellular addresses, such as through the incorporation of discrete localization tags, thereby enabling selective observation of signaling dynamics at distinct locations in the cell. The ongoing development and application of FP-based biosensors over the last few decades has thus had a transformative impact on the study of signaling microdomains, offering an unparalleled window into their properties and regulation that begins to reveal their true biological significance.

In this review, we first provide an overview of the basic principles of FP-based biosensor design and then discuss how biosensors are helping to advance our understanding of signaling microdomains and their underlying regulatory mechanisms. Although there is still no clear classification of signaling microdomains, for the purpose of discussion, we group currently reported microdomains into three classes based on their assembly characteristics according to current knowledge: 1) Membrane-delimited signaling microdomains, 2) signaling microdomains established through regulatory “fences” and 3) microdomains formed through the assembly of signaling molecules.

Genetically Encoded Fluorescent Biosensors

Fluorescence has long been recognized as a valuable tool to permit detailed examination of molecular and cellular phenomena (4), and countless fluorescent probes of varying designs have been generated throughout the past century. The advent of genetically encoded fluorescent probes, facilitated by the cloning of green fluorescent protein (GFP) and the systematic engineering of the FP superfamily at the turn of the millennium (5, 6), transformed the development of these molecular tools by enabling the construction and delivery of optical probes using straightforward recombinant DNA techniques.

Conceptually, the design of a fluorescent biosensor involves coupling a sensing unit that can detect a given biochemical event to a reporting unit that is responsible for producing the optical readout. In a genetically encoded, FP-based biosensor, the sensing unit is often derived from endogenous cellular components (i.e., protein sequences) that natively participate in the pathway of interest, while the reporting unit consists of one or more FPs fused to the sensing unit, such that the signaling input to the sensing unit alters the fluorescence output of the FP. Below, we illustrate these concepts by discussing several key biosensor classes. A more extensive accounting of the multitude of biosensor designs, targets, and fluorescence readouts that have been reported can be found in a recent review by Eric Greenwald and coworkers (7), as well as online via our Fluorescent Biosensor Database (biosensordb.ucsd.edu).

Passive reporters

Similar to the practice of using FPs to tag proteins of interest, many simple biosensor designs utilize the reporting unit as a passive bystander, with the fluorescent signal merely highlighting the presence or location of the sensing unit within the cell. Because FPs generally adopt the intrinsic subcellular localization of the sensing unit, **passive reporters** can likewise be used to “tag” signaling molecules that the sensing unit binds and localizes to. For example, phosphoinositides, which are critical lipid messengers produced in cellular membranes (8), engage in signaling through the binding of lipid-binding domains and recruitment of effector proteins that contain these domains (9, 10). Thus, by fusing an FP to one such lipid-binding domain, the production or depletion of these phospholipid messengers can be visualized according to the translocation of the biosensor to or from specific cellular membranes. Early applications include the work of Péter Várnai et al. and Alexander Gray et al., who tagged the pleckstrin homology domains of PLC δ , Akt and GRP1 with GFP to selectively monitor the dynamics of PI(4,5)P $_2$ and PI(3,4,5)P $_3$ signaling (11, 12). One limitation of this translocation-based design is its dependence on natively occurring protein domains to generate the sensing unit. Thus, in addition to the use of endogenous proteins, various sensors are also being developed using nanobodies (13), which are well-suited for visualizing signaling molecules in living cells owing to their exquisite specificity, small size, high solubility, and stability. Potential uses of nanobodies to probe signaling have been widely reported, including the dynamic tracking of endogenous proteins (14–16), as well as the development of conformation-sensitive fluorescent reporters that can selectively highlight the active forms of signaling proteins (17, 18). Another recent innovation is the development of engineered sensing units that translocate to a specific subcellular compartment upon sensing the biochemical event of interest, rather than translocating to the signal itself, an approach that enables visualizing the activity of protein kinases through biosensor translocation (19, 20).

Active reporters

Whereas the fluorophore in a passive reporter is not directly affected by the sensing unit, an alternative design strategy involves actively coupling the fluorescence properties of the reporting unit to the molecular state of the sensing unit, which takes the form of a molecular switch that undergoes a conformational change in response to a target biochemical input. The fluorophore of an **active reporter** is thus sensitized to the “on” and “off” states of

the molecular switch. Depending on the specific configuration of the sensing and reporting units, this can lead to modulation of FP photophysical characteristics including fluorescence intensity, spectrum, lifetime and even photochromism, as a readout for signaling pathway dynamics. The switch itself can be derived from the intrinsic conformational switches present in many native proteins or engineered from isolated domains that are linked together. Given the diversity of molecular switches and the variety of fluorescent readouts, active reporters are by far the largest and most diverse class of FP-based biosensors, capable of reporting on a wide range of signaling events.

Single-fluorophore biosensors—A straightforward approach to controlling FP fluorescence is to integrate a molecular switch directly within the β -can of a single FP, as distortion of the FP structure by the switch conformation will alter the local environment of the fluorophore. This process was initially demonstrated through the development of genetically encoded calcium indicators (GECIs). Geoffrey Baird and coworkers generated *camgaroo1* by inserting *Xenopus laevis* calmodulin (CaM) into EYFP, whereby the binding of calcium ion (Ca^{2+}) causes CaM to adopt a compact conformation that enhances fluorescence intensity (21). Nagai et al. and Nakai et al. subsequently generated *pericam* (22) and *GCaMP* (23) by inserting both CaM and the myosin light chain kinase-derived M13 peptide into circularly permuted YFP (cpYFP) and cpGFP respectively. Including the CaM-binding M13 peptide enables a more robust conformational change in the presence of Ca^{2+} . This strategy has since been adapted to yield numerous other genetically encoded indicators for visualizing membrane potential (24–26), second messengers such as cAMP (27–30) and cGMP (31, 32), metabolites (33, 34), neurotransmitters (35–37), and even protein kinase activity (38). Though most of these sensors exhibit a change in FP fluorescence intensity at a single wavelength in response to their specific signaling input, others in fact show a spectral shift between two different wavelengths. For example, ratiometric *pericam* shifts its preferred excitation wavelength from 415 nm to 495 nm upon calcium binding, and the biosensor response is read out as the ratio of fluorescence intensity at these two wavelengths (22). Similar excitation-ratiometric responses are observed with the GECIs *GEX-GECO1* and *REX-GECO1* (39) and the NADPH sensor *iNap* (40), as well as our recently developed series of excitation-ratiometric kinase activity reporters (*ExRai-KARs*) (38). Meanwhile, another GECI, *GEM-GECO1*, shifts its emission wavelength from 450 nm to 510 nm upon Ca^{2+} binding (39). Though somewhat more technically demanding to measure, ratiometric responses are advantageous for cancelling out some of the experimental variations that can interfere with single-wavelength imaging (e.g., differences in probe expression, cell thickness, or illumination intensity) (41).

Multi-FP biosensors: Along with engineered modulation of the fluorophore environment, the fluorescence of an FP can also be affected by the presence of a second FP in close proximity. Many sensors therefore take advantage of this design principle by incorporating a pair of FPs as the reporting unit such that the molecular switch will alter the relative distance and orientation between the FPs and hence the fluorescence readout. The most widely utilized example of this approach are sensors based on Förster resonance energy transfer (FRET). FRET is an electrodynamic phenomenon of radiationless energy transfer from an excited-state donor fluorophore (e.g., FP) to a ground-state acceptor fluorophore via

dipole-dipole coupling (42). In addition to depending on photophysical properties such as donor quantum yield, acceptor extinction coefficient, and overlap between donor emission and acceptor absorption spectra, FRET efficiency is exquisitely sensitive to the relative distance and orientation between donor and acceptor (42, 43), making the FRET change between an FP pair an excellent reporter of conformational changes within a molecular switch.

The earliest FRET-based biosensors included the very first GECI. Specifically, while working with Roger Tsien, Atsushi Miyawaki constructed the Ca^{2+} indicator cameleon by sandwiching a Ca^{2+} -sensitive molecular switch consisting of CaM linked to the aforementioned M13 peptide between the FRET pair of BFP and GFP (44). The reversible binding of Ca^{2+} to CaM induces the binding of CaM to M13, and the ensuing conformational change in the molecular switch alters the proximity of the two FPs, and thus the FRET efficiency between them. A subsequently improved version, yellow cameleon, incorporated CFP and YFP as a much more efficient FRET pair (45) and became the template for nearly all subsequent FRET-based biosensor designs. Numerous FRET-based biosensors have since been developed to monitor the dynamics of other metal ions such as zinc (46, 47) and intracellular messengers such as cAMP (48–50), cGMP (51–53), and phosphoinositides (54–56). The dynamics of enzyme activity can also be revealed using this approach. Many genetically encoded kinase activity reporters (KARs), for instance, utilize an engineered molecular switch wherein the consensus phosphorylation sequence for a specific kinase is linked to a phosphoamino acid-binding domain (PAABD) and sandwiched between an FP pair. Phosphorylation of the peptide by the kinase of interest triggers binding by the PAABD, resulting in a conformational change that can be captured by FRET. Various FRET-based KARs have thus been generated for different kinases such as PKA (57, 58), PKC (59, 60), PKB/Akt (61), ERK (62), Aurora kinase (63), and many others (7). Similarly linking a given GTPase to the binding domain from an effector has yielded numerous reporters for visualizing GTPase signaling dynamics in cells (64–66). Because FRET induces reciprocal changes in the emission intensity of the acceptor and donor FPs upon donor excitation, FRET biosensor responses are commonly read out as the acceptor-to-donor emission ratio. However, FRET also affects other photophysical properties of FPs that enable additional readout modalities. Notably, FRET decreases the lifetime (τ) of the donor FP excited state, which can be monitored via fluorescence lifetime imaging (67). FRET also affects the polarization of emitted light following polarized excitation, which can be measured using fluorescence anisotropy imaging. This phenomenon recently yielded a family of fluorescence anisotropy reporters based on homoFRET, or FRET between two spectrally identical fluorophores (60).

Signaling Microdomains Illuminated by Fluorescent Biosensors

With their dynamic readout, adaptable designs, and non-invasive nature, genetically encoded FP-based biosensors have proven to be ideal tools for tracking biochemical processes within the native cellular context. The formation of signaling microdomains has long been hypothesized to play a central role in the spatial regulation of intracellular signaling networks, and decades of research using FP-based biosensors have yielded invaluable insights into the mechanisms and functions of these minute signaling compartments. In this

section, we discuss how the use of FP-based biosensors and live-cell imaging approaches are illuminating the organizing principles that govern signaling microdomains and revealing the molecular processes that define their various boundaries: 1) association with membrane-delimited structures; 2) dynamic “fencing” by regulatory factors; and 3) assembly of multi-component molecular complexes.

Membrane-delimited signaling microdomains

Microdomains formed by membranes—Physical compartmentation of the cell interior by various membrane structures imposes numerous layers of spatial control over biochemical processes. Membrane-bound organelles, for instance, form functionally specialized subcellular compartments with distinct regulatory landscapes that provide various unique platforms for compartmentalizing the actions of signaling molecules, and such spatial heterogeneity can be elucidated using FP-based biosensors.

For example, G-protein-coupled receptors (GPCRs) are known to mediate signaling from the cell surface by regulating the production of second messengers such as cAMP. This “canonical” GPCR signaling has long been thought to occur exclusively at the plasma membrane (PM) and cease when receptors undergo clathrin-mediated endocytosis following β -arrestin binding. However, parallel work by Davide Calebiro et al. and Sébastien Ferrandon et al. called into question the conventional wisdom on canonical GPCR signaling by using FRET-based cAMP indicators to show that internalized thyroid stimulating hormone receptor (TSHR) (68) and parathyroid hormone receptor (PTHr) (69) remain active and promote sustained cAMP signaling from the endosomal surface. In a subsequent study, Roshanak Irannejad and colleagues directly examined the subcellular distribution of beta2-adrenergic receptor (β 2AR) activation using the nanobody-based translocation sensor Nb80-GFP (17). This sensor, which selectively recognizes the active form of β 2AR, translocates from the cytosol to the PM upon isoproterenol stimulation of β 2AR. However, following prolonged stimulation, Nb80-GFP relocates to intracellular puncta containing internalized, endosomal β 2AR, elegantly highlighting the distinct phases of β 2AR signaling occurring in different organelles (17). In addition to endosomes, recent studies using FRET-based cAMP indicators have detected internalized TSHR and β 1AR signaling on the Golgi membrane (70, 71), while the use of translocation-based sensors has also shown that Golgi-localized β 1AR activity induces a local signaling axis to direct Golgi PI4P depletion (72). Combined, these studies exemplify the rapidly evolving paradigm of spatial GPCR signaling (73).

Subcellular targetability is a key feature of genetically encoded biosensors that can be used to greatly enhance the spatial selectivity of biosensor-based studies. By localizing FP-based biosensors to different cellular membranes, researchers have been able to explore the distinct biochemical microenvironments that surround various organelles and reveal that specific biochemical pathways can exhibit dramatically different subcellular activity patterns (74–77). Recently, Xin Zhou and colleagues applied this strategy to investigate the spatial regulation of mechanistic target of rapamycin (mTOR) complex 1 (mTORC1) (78). The serine/threonine protein kinase mTORC1 serves as a central hub connecting nutrient signaling and cell growth with a wide range of environmental inputs (79). Although

mTORC1 has been reported to associate with different subcellular compartments, the role of such spatial compartmentation in regulating mTORC1 signaling is still quite unclear. To address this question, Zhou et al. constructed a first-generation FRET-based mTORC1 activity reporter (TORCAR) by sandwiching the translation initiation factor 4EBP1, a known mTORC1 substrate, between CFP and YFP (78). Using subcellularly targeted variants of TORCAR, they successfully detected local mTORC1 activity in different subcellular regions, including the nucleus, where the existence of mTORC1 signaling remains controversial. Notably, the authors also observed differential regulation of subcellular mTORC1 in response to different inputs, with growth factor stimulation inducing mTORC1 activity throughout the cell while nutrient sensing selectively induced lysosomal and nuclear mTORC1 activity, providing important insights into the regulation of mTORC1 signaling by membrane compartments.

Microdomains formed between membranes—While the compartmentalization of biochemical processes within distinct membrane-bound organelles has obvious advantages for organizing eukaryotic cellular functions, it also poses challenges for the coordinated regulation of these activities, requiring mechanisms for inter-organelle communication. Indeed, the established view of intracellular organelles as discrete, isolated entities is being upended by an emerging reality that recasts organelles as dynamic, interactive bodies that communicate through the close juxtaposition (e.g., 10–80 nm) of organelle membranes to allow molecular exchange without direct organelle fusion (80, 81). Although these membrane contact sites (MCSs) were initially observed by early electron microscopists (82, 83), it wasn't until the recent development of more advanced imaging tools, including FP-based biosensors, that the unique molecular features and specialized signaling function of these submembrane microdomains could begin to be elucidated.

Since MCSs are small in size and quite dynamic, directly targeting genetically encoded biosensors to these sites is an ideal strategy to study these relatively transient microdomains in the cellular context. For example, cardiac contraction is regulated by intracellular Ca^{2+} release within the dyad, a membrane subdomain formed between the sarcoplasmic reticulum (SR) and sarcolemma (84). Given that whole-cell Ca^{2+} transients associated with cardiac excitation-contraction coupling represent the sum of roughly 10^4 Ca^{2+} sparks within dyads, Wei Shang and colleagues sought to investigate the dynamics and regulation of elemental Ca^{2+} release events within these MCSs by fusing GCaMP6f (85), a highly sensitive GECI with fast kinetics and high affinity, to the dyad junctional proteins junctin 1 and triadin (Figure 1) (86). Both targeted sensors co-localized with ryanodine receptors (RyRs) within discrete puncta corresponding to dyadic clefts. These targeted sensors allowed the authors to observe spontaneous “nanosparks” corresponding to rapid Ca^{2+} transients from single dyads, including the operation of distinct RyR clusters within a dyad (86). Nanosparks displayed much higher amplitudes compared with global Ca^{2+} elevations, directly highlighting the distinct signaling environment formed within these microdomains. By faithfully recording the timing of these Ca^{2+} release events, this strategy should facilitate deeper investigation into aberrant Ca^{2+} dynamics in diseases associated with dyssynchronous Ca^{2+} release, such as heart failure and cardiac arrhythmia.

Moo Yeol Lee and coworkers employed a similar strategy to investigate plasma membrane and sarco/endoplasmic reticulum (S/ER) contact sites (87). As with cardiac and skeletal myocytes, PM-S/ER junctions are thought to play a key role in regulating Ca^{2+} signaling and homeostasis in neurons, glia, and smooth muscle cells (88). By fusing GCaMP2 to the sodium pump $\alpha 2$ catalytic subunit, which localizes to the PM face of these submembrane microdomains (89), or to the $\alpha 1$ catalytic subunit, which is more evenly distributed in the PM, the authors were able to probe spatial control of junctional Ca^{2+} signals. While both targeted sensors reported Ca^{2+} elevations in control cells treated with 5HT (smooth muscle) or ATP (astrocytes), only $\alpha 2$ -fused GCaMP2 responded in cells loaded with the Ca^{2+} chelator EGTA, which buffers global Ca^{2+} increases, thus revealing a spatially distinct Ca^{2+} microdomain at these MCSs (87).

A different strategy was applied by Amit Agarwal and colleagues to identify Ca^{2+} microdomains formed between branched membrane processes and mitochondria in astrocytes, which are thought to be important for facilitating local homeostasis of neural circuits (90). In this study, the authors monitored spontaneous Ca^{2+} transients in acute brain slices from transgenic mice expressing membrane-anchored GCaMP3 (91) (mGCaMP3) only in astrocytes. Despite localizing throughout the PM, mGCaMP3 nevertheless revealed discrete Ca^{2+} spikes in individual microdomains. The authors then used a custom machine-learning algorithm for Ca^{2+} signal classification and decoding (CaSCaDe) to automatically segment, analyze, and map active Ca^{2+} microdomains in all astrocytes within a slice. Using this approach, the authors characterized the dynamics of these Ca^{2+} microdomains and also traced their origin. Importantly, these Ca^{2+} microdomains were found to colocalize with mitochondria, which were also enriched in astrocyte branches and closely juxtaposed with the PM. Meanwhile, blockade of the mitochondrial permeability transition pore, which can trigger fast mitochondrial Ca^{2+} release (92), dramatically reduced the frequency, duration, and amplitude of microdomain Ca^{2+} spikes, identifying mitochondria as the Ca^{2+} source. Functional assays also showed that superoxide and high extracellular glucose can enhance microdomain Ca^{2+} signals, suggesting that mitochondria are able to integrate changes in ROS and metabolic status to regulate astrocyte Ca^{2+} signaling (90). Given that astrocyte Ca^{2+} transients are altered by nervous system injury and disease (93), future work in this area may offer crucial insights into pathological mechanisms.

Microdomains formed within membranes—Compartmentalized signaling subdomains on the order of tens to hundreds of nanometers in size can also form within individual cellular membranes through both transient and stable interactions between membrane constituents. A particularly well-known example involves the selective partitioning of cholesterol- and sphingolipid-rich regions of the plasma membrane into so-called membrane “rafts” that serve as specialized platforms for organizing various biochemical processes, including signaling pathways (94, 95). While the submicron scale of these membrane subdivisions generally precludes direct observation in living cells, the spatial selectivity of biosensor targeting is often used to reveal their role in signaling compartmentation.

For example, a series of studies over the past decade have utilized lipid-modification sequences known to direct proteins to different membrane microdomains (96) in conjunction

with FP-based biosensors to examine spatial control of the growth factor-stimulated PI3K/Akt pathway, which is known to be linked to membrane rafts (94, 97). Using a FRET-based Akt kinase activity reporter, Xinxin Gao and co-workers found that platelet-derived growth factor (PDGF) stimulation preferentially induced Akt activity in membrane rafts compared with non-raft regions (98). A follow-up study by Gao et al. then used a similarly microdomain-targeted FRET sensor for measuring the activation of PDK1, an upstream activator of Akt, to reveal that PDGF treatment induces PDK1 activation solely in membrane rafts, due to the exclusion of the negative regulator PTEN from these regions (99). This finding is supported by recent work from Jihye Seon and colleagues, who applied this targeting strategy to a FRET-based sensor for monitoring the activity of the PDGF receptor (PDGFR) itself (100). PDGFR was found to be uniformly activated in both raft and non-raft membrane regions following PDGF stimulation, confirming that the differential regulation of downstream cascades in different membrane microdomains is responsible for PI3K/Akt pathway compartmentation.

Besides lipid partitioning, studies are increasingly showing that clustering of transmembrane proteins such as cell surface receptors can also drive the formation of plasma membrane microdomains that function as discrete signaling islands (101). For example, clustered T-cell receptors (TCRs) are thought to serve as signaling platforms that initiate and amplify TCR signaling during T-cell activation (102). To directly probe the dynamics of TCR clustering and begin investigating their role in T-cell signaling, Yuanqing Ma and colleagues developed the FRET-based sensor CliF (clustering reported by intermolecular FRET), in which the FRET pair YFP and RFP is tethered to the cytoplasmic tail of a specific receptor such that changes in clustering will be reported as changes in intermolecular FRET between CliF modules (103). Both FPs are truncated to remove their flexible termini and also joined with a two-amino acid linker, thus minimizing the contribution from intramolecular FRET changes. By applying CliF to the TCR co-receptor CD3 ζ , they were able to observe stimulus-dependent differences in TCR cluster density and mobility within the immunological synapse. These differences in TCR cluster dynamics and remodeling may account for differences in the timing and duration of TCR signaling.

Signaling microdomains established through regulatory “fencing”

While intrinsic subcellular compartments provide ready-made staging platforms for spatially defined signaling, cells must utilize additional mechanisms to locally confine the actions of signaling molecules that might otherwise diffuse freely throughout the cell interior. Studies using genetically encoded biosensors are revealing that, by delicately balancing the forces controlling the local concentrations of active signaling molecules, such as production, degradation, and buffering, cells can establish dynamic regulatory boundaries that “fence in” signaling molecules and give rise to diverse signaling microdomains.

Locally concentrated channels, transporters and enzymes that produce signaling molecules can generate “hot spots” of highly concentrated signaling activity. For instance, the existence of a cAMP microdomain around the Ca²⁺-stimulated adenylylate cyclase (AC) isoform AC8 was detected by using a targeted cAMP indicator, suggesting the possibility that ACs, the source of cAMP production, can be primary architects of cAMP signaling

microdomains (104). To detect local fluctuations in cAMP caused by endogenous AC8 activity, Sebastian Wachten and colleagues tagged the catalytically dead AC8^{D416N} mutant with the cAMP sensor Epac2-camps (49). By contrasting the response of this sensor with that of diffusible or globally PM-targeted Epac2-camps, the authors found that thyrotropin-releasing hormone-triggered Ca²⁺ release in GH₃B₆ pituitary cells specifically elevated cAMP levels near AC8 while at the same time suppressing global cAMP levels by inhibiting AC5 and AC6 (104). Applying a similar strategy, Debbie Willoughby and coworkers used the Ca²⁺ sensor GCaMP2 (105) fused to either AC2 or AC8 to also reveal the presence of a distinct Ca²⁺ microdomain around AC8 that was specifically responsive to capacitative Ca²⁺ entry (106). These results suggested the existence of a finely tuned Ca²⁺-dependent cAMP microdomain where the sources of cAMP and Ca²⁺ are in close proximity.

Conversely, signaling microdomains can be shaped by the formation of “sinks” in which signaling molecule concentrations are locally suppressed via degradation or buffering. For example, cAMP is degraded into AMP by a family of enzymes called phosphodiesterases (PDEs), and work by Christian Lohse and colleagues recently demonstrated using a PDE-targeted cAMP sensor that individual PDE molecules can effectively generate low-cAMP zones in their immediate vicinity (107). Indeed, cAMP degradation by PDEs has long been implicated as a prominent force responsible for setting the bounds of cAMP microdomains by preventing cAMP from diffusing out of or into different signaling compartments (108, 109). This fencing ability was recently illustrated in work by Terri Clister and coworkers investigating the regulation of nuclear cAMP/PKA signaling (Figure 2) (110). Directly targeting the FRET-based cAMP indicator ICUE3 (111) to a nuclear-localized A-kinase anchoring protein (AKAP), AKAP95, revealed a microdomain in the immediate vicinity of AKAP95 that was insulated from cAMP signals originating from the PM, despite clear elevations in overall nuclear cAMP levels under the same conditions. In contrast, selectively inducing cAMP production from within the cytosol led to cAMP elevations in both the general nucleus and AKAP95 microdomain. Further investigation revealed that AKAP95 forms a complex with PDE4D5 and that PDE4D5 inhibition abolishes the fence surrounding AKAP95, allowing PM-generated cAMP to penetrate this microdomain (110). Given the previously established existence of a resident pool of nuclear PKA (112), this work identifies the regulatory framework through which cells avoid spurious activation of nuclear PKA by PM-derived cAMP while enabling selective activation by cytosolically generated cAMP, such as that triggered by internalized GPCRs (see above).

Modulating the balance among production, degradation, and diffusion enables cells to promote global biochemical heterogeneities in the form of signaling gradients. For instance, early studies using translocation-based sensors for 3-phosphoinositides (3-PIs; e.g., PI[3,4,5]P₃, PI[3,4]P₂) revealed that chemotaxing cells exhibit a sharp gradient of 3-PI production directed toward the leading edge of the plasma membrane (113, 114). Formation of these gradients was found to be partially regulated by PI3K and PTEN, which produce and degrade 3-PIs, respectively, and localize oppositely along the front and rear of migrating cells (115). A recent study using a membrane-targeted version of the Ca²⁺ indicator R-GECO1 (39) revealed a gradient of Ca²⁺ sparklets oriented toward the rear of cells migrating in response to fibroblast growth factor receptor (FGFR) activation (116). The authors hypothesized that this Ca²⁺ gradient was due to the asymmetric activation of

L-type voltage-dependent Ca^{2+} channels (LTCCs) toward the rear of the cell. LTCC activity is regulated by two pathways downstream of FGFR, namely, PI3K and PKC. Kim et al. found that the rapid rearward diffusion of 3-PIs produced by PI3K at the cell front, where FGFR is activated, stimulates LTCC activity at the back of the cell, while PKC enriched at the front of the cell simultaneously inhibits LTCC activity in this region. These antagonistic pathways elicit site-specific effects through signal coupling in the leading or trailing regions of a single cell, yielding a rear-oriented pattern of Ca^{2+} sparklets (116).

Asymmetries in the production and degradation of cAMP were similarly shown to play an important role in forming signaling gradients during polarized growth in hippocampal neurons. In a study using untargeted ICUE3, Kirill Gorshkov and coworkers observed a gradient of increasing cAMP levels that was oriented towards the elongating axon, which resulted from high PDE/low AC activity in the soma and proximal axon versus high AC/low PDE activity in the distal axon (117). Work by Isabella Maiellaro and colleagues also revealed a high degree of cAMP compartmentalization in *Drosophila* motor neurons expressing the cAMP sensor Epac1-camps. Specifically, the authors observed cAMP elevations that were confined within individual synaptic boutons following localized neurotransmitter application (118). Little response was detected from the axon and soma, and this was found to arise from the absence of receptor expression, and thus cAMP production, in the axon and high PDE accumulation in the cell body. Interestingly, high levels of PDE expression were also observed within the processes joining neighboring boutons, thereby preventing cAMP diffusion between boutons. The highly polarized and intricate morphology of neurons lends itself to compartmentalized signaling (119), and biosensor-based studies have even indicated that cellular geometry can directly influence the production and degradation of signaling molecules to yield microdomains. For example, the high surface-to-volume ratio of narrow dendritic processes has been shown to yield cAMP gradients simply by virtue of the fact that cAMP is largely produced by PM-embedded ACs and degraded by cytosolic PDEs (120).

Microdomains formed through the assembly of signaling molecules

Cells contain hundreds of different signaling molecules, which make up nearly 10% of all expressed proteins (121). Yet signaling pathway function critically depends on the ability of the correct molecular players to reliably find one another and react productively amidst a crowded molecular background. Thus, cells frequently use protein-protein interactions to coordinate the activities of pathway components by assembling them into dynamic molecular complexes. For example, imaging studies using FP-tagged enzymes have revealed the existence of protein complexes termed “purinosomes” (122) and “glucosomes” (123) in which key enzymes involved in *de novo* purine biosynthesis and glucose metabolism, respectively, assemble into molecular machines. Along these lines, detailed live-cell imaging studies using FP-based biosensors are increasingly shedding light on how multi-protein assemblies impose additional layers of spatial control over signaling activity.

The assembly of signaling molecules into protein complexes is often accomplished in cells through the use of multivalent scaffolds, which coordinate signaling activities by tethering different protein partners together, anchoring them to specific subcellular locations

and downstream targets, and even directly modulating the behavior of bound enzymes (124, 125). Spatial compartmentation of PKA signaling in particular is tightly regulated by AKAPs, which comprise the most extensively studied family of scaffold proteins (126), and numerous studies have revealed that AKAP complexes form unique signaling microdomains. For example, by fusing different binding domains derived from mAKAP to the FRET-based PKA activity reporter AKAR, Kimberly Dodge-Kafka and colleagues were able to directly visualize the coordinated interplay among PDE4D3, ERK5, the cAMP-activated guanine nucleotide exchange factor Epac1, and Rap1 GTPase in shaping the local activity dynamics of co-anchored PKA (127). Besides PKA and PDE4D3, mAKAP is known to bind AC2 and AC5, which it recruits into a signaling complex on the cytosolic surface of nuclear envelope (128) to form a self-contained perinuclear microdomain (Figure 3). Tomasz Boczek and coworkers were able to directly visualize PKA signaling within this compartment by fusing AKAR to nesprin-1 α , the protein responsible for bringing mAKAP to the nuclear envelope (129). By selectively perturbing local cAMP production and degradation, they were also able to show that mAKAP-anchored PKA signaling is necessary and sufficient to promote axon growth in hippocampal neurons, and that anchored PDE activity was responsible for tuning microdomain signaling activity.

The importance of molecular scaffolds extends well beyond PKA signaling. For example, by using scaffold-targeted forms of the FRET-based PKC activity reporter CKAR (59), along with isoform-selective kinase inhibitors, Tobias and Newton showed that the atypical PKC isoform PKC ζ is allosterically activated upon binding by the scaffold proteins p62 and PAR6 (130). Numerous molecular scaffolds are also known to participate in the regulation of MAP kinase cascades (131). The Shoc2 protein, for instance, has been shown to facilitate Ras/Raf/MEK/ERK signaling by scaffolding the Ras-Raf interaction (132). However, work by Sayaka Yoshiki and colleagues also identified a role for Shoc2 in mediating the co-regulation of Raf-1 activity by Ca²⁺ signaling. Specifically, they used the FRET-based Raf-1 biosensor Prin-Raf1 (133) to demonstrate that Ca²⁺ signaling enhances Raf-1 activation by displacing CaM from Shoc2, thereby promoting Ras binding (134). Rie Matsunaga-Udagawa and co-workers similarly used a FRET-based Ras-Raf-1 interaction sensor in conjunction with computational modeling to tease apart the kinetic impact of scaffolding on this pathway, revealing that Shoc2 accelerates, rather than stabilizes, the Ras-Raf interaction (135).

Genetically encoded FP-based biosensors clearly provide useful insights into the role of molecular assemblies in generating and shaping signaling microdomains, yet the limitations of conventional fluorescence microscopy obscure many of the finer spatial details associated with these submicron compartments. Thus, while current approaches allow researchers to infer the behavior of signaling microdomains, alternative methods are needed to directly visualize the molecular-scale compartmentation of signaling activities. To this end, Gary Mo and colleagues devised a biosensing strategy based on a novel phenomenon known as Fluorescence fLuctuation INcrease by Contact (FLINC), wherein the red FP TagRFP-T exhibits increased fluorescence intensity fluctuations (i.e., blinking) when brought into close proximity to the green FP Dronpa, to directly observe the compartmentation of dynamic signaling activities in super-resolution (136). Specifically, by linking Dronpa and TagRFP-T together using the PKA-dependent molecular switch found in AKAR (57), they were able to

couple changes in PKA activity to changes in TagRFP-T blinking behavior. When imaged in combination with a fluctuation-based super-resolution imaging technique known as photochromic stochastic optical fluctuation imaging (pcSOFI) (137), the resulting FLINC-AKAR sensor revealed the presence of nanometer-sized domains of kinase activity along the PM of HeLa cells following PKA stimulation (136). Additional super-resolution imaging and co-localization studies demonstrated that these kinase activity puncta corresponded to discrete clusters of AKAP79-scaffolded PKA at the PM, thereby offering an unprecedented glimpse of the intricate signaling architecture formed by molecular complexes.

Applications Beyond Signaling

Although FP-based biosensors have predominantly been used to visualize the spatiotemporal regulation of intracellular signaling, they are increasingly being utilized for more translational applications. Indeed, dysregulated signaling is a factor in numerous diseases, and many signaling molecules are important drug targets. The ability of biosensors to track biochemical processes in real time thus lends itself to investigating the spatiotemporal dynamics of drug action. For example, Max Nobis and colleagues used a FLIM-FRET Src biosensor to monitor the efficacy of dasatinib, a Src inhibitor, in a transgenic mouse model of pancreatic cancer (138). Specifically, they were able to track dasatinib clearance from the tumor microenvironment through the recovery of Src activity, while greater Src activity at increasing distance from the blood supply also revealed limited dasatinib penetration in deep tumor tissues. Tatsuaki Mizutani and colleagues similarly utilized a FRET-based biosensor for Bcr-Abl (Pickles), a fusion kinase expressed in chronic myeloid leukemia (CML), to monitor the efficacy of various tyrosine kinase inhibitors (139). Drug resistance caused by Bcr-Abl mutations poses a growing therapeutic challenge for CML, and the authors were able to detect heterogeneous responses to both first- and second-generation drugs in cells expressing Bcr-Abl mutants. Introducing Pickles into mononuclear cells from CML patients further enabled drug efficacy predictions for individual patients, a strategy that has recently been applied for pretreatment evaluations of the clinical efficacy and safety of dasatinib (140) and nilotinib therapy (141).

Improvements in biosensor signal-to-noise ratio (SNR) are also enabling their application to high-throughput drug screening efforts. For instance, Yuzheng Zhao and colleagues recently developed a high-SNR genetically encoded sensor, SoNar, for tracking cytosolic NAD⁺ and NADH redox states that allowed them to screen >5,500 unique compounds for new agents targeting tumor metabolism (142). They ultimately identified KP372-1, a previously reported Akt inhibitor, which induced extreme oxidative stress and showed selective toxicity to tumor cells in vivo by targeting NQO1-mediated futile redox cycling, which is specifically activated in various cancers. A recent screening effort by Yasna Contreras-Baeza and colleagues also suggests that FP-based biosensors can be used for pre-clinical toxicity testing. Using a FRET-based lactate biosensor, Laconic (143), to monitor lactate accumulation induced by mitochondrial toxicants, the authors performed a pilot screen in Laconic-expressing MDA-MB-231 cells using commercial drugs that were previously withdrawn from the market due to liver/cardiac toxicity issues (144). This approach consistently reported the known cellular toxicities identified for these molecules,

highlighting a potential strategy for direct assessment and early detection of mitochondrial toxicity in the drug development pipeline, thus helping save time, money, and lives.

Current Limitations and Future Improvement

While the above examples illustrate the growing utility of genetically encoded biosensors to illuminate the spatiotemporal dynamics of intracellular biochemistry, there are still various limitations that must be taken into consideration when using fluorescent biosensors. One frequent concern is the risk of perturbing endogenous signaling events. For instance, the molecular switches of many sensors are derived from native proteins that may titrate or buffer endogenous molecules when overexpressed. The use of subcellularly targeted sensors where localization is achieved by directly tagging the biosensor to a protein of interest can lead to similar concerns related to signaling protein overexpression. Improvements in FP brightness and biosensor SNR can help alleviate some of these concerns by providing robust signals at lower expression levels, while the use of genome-editing techniques to directly express tagged sensors from endogenous genomic loci might offer another potential solution. Nevertheless, rigorous controls and orthogonal approaches remain critical to ensure that biosensor expression does not alter the pathway(s) being studied.

Another ongoing challenge is the use of FP-based biosensors for in vivo applications, which is limited due to the fact that the fluorescence of most commonly used FPs cannot penetrate well in tissues primarily due to light scattering. Because wavelengths in the near-infrared (NIR) region of the spectrum are less prone to absorption and scattering in mammalian tissues, a common strategy to facilitate in vivo biosensor applications is the use of multiphoton excitation, which enables tissue and in vivo imaging of standard FP-based biosensors using long-wavelength illumination (145). This approach is often used in combination with single-FP sensors such as the Ca^{2+} indicator GCaMP6 (85) and the voltage indicator ASAP3 (25), as well as with FLIM-FRET sensors for enzyme activity (58, 138). Meanwhile, considerable efforts are also being applied to the development and optimization of FP variants that are excited and emit light at NIR wavelengths (6), and to generate fluorescent biosensors based on these NIR-FPs. Recent efforts have already yielded single-FP biosensors for monitoring caspase activity (146) and calcium dynamics (147), as well as NIR variants of cyan/yellow FRET-based biosensors for monitoring GTPase (Rac1) and kinase (PKA, JNK) activities (148).

Concluding Remarks

Genetically encoded biosensors have already proven themselves to be powerful tools capable of illuminating the landscape of intracellular signaling, yielding innumerable insights into the molecular logic of compartmentation of signaling activities and the formation of diverse signaling microdomains. Over the past two decades, our view of compartmentalized signaling has expanded in parallel with the sophistication of the FP-based imaging toolkit, and the recent demonstration of dynamic super-resolution activity imaging using FLINC-based biosensors (136), as well as the development of new automated analytical workflows such as CaSCaDe (90), highlight the continuing technological advances that promise to further deepen our understanding in the future. Meanwhile, entirely new kinds of signaling

microdomains await detailed investigation using FP-based biosensors. In particular, the recent emergence of liquid-liquid phase separation, and the consequent formation of “membraneless organelles”, as a general means of organizing biochemical activities within discrete compartments in cells (149, 150) is expected to have significant implications for the spatial regulation of signaling, given that the intrinsic disorder and multivalent binding that characterize these biomolecular condensates are also common motifs in signaling pathways (151, 152). FP tagging has already greatly facilitated the study of phase separation in situ, and we anticipate that future investigations utilizing biosensors in place of these passive highlighters will directly reveal the impact of phase separation on signaling activities. Genetically encoded FP-based biosensors thus remain a guiding light on the frontiers of signal transduction research.

Acknowledgements

This work is supported by the National Institutes of Health (R01 MH111516, R35 CA197622, R01 DK073368, and R01 GM111665 to J.Z.) and the Air Force Office of Scientific Research (FA9500-18-1-0051 to J.Z.).

Abbreviations and Definitions

BFP

blue fluorescent protein

CFP

cyan fluorescent protein

GFP

green fluorescent protein

RFP

red fluorescent protein

YFP

yellow fluorescent protein

EYFP

enhanced yellow fluorescent protein

4EBP1

eukaryotic translation initiation factor 4E binding protein 1

AKAR

A-kinase activity reporter

CD

cluster of differentiation

CKAR

C-kinase activity reporter

cAMP

3',5'-cyclic adenosine monophosphate

cGMP

3',5'-cyclic guanosine monophosphate

Epac

exchange protein directly activated by cAMP

ICUE

indicator of cAMP using Epac

PI3K

phosphoinositide 3-kinase

PDK1

phosphoinositide-dependent kinase 1

Pickles

phosphorylation indicator of CrkL *en* substrate

PAR6

partitioning defective 6

PKA

protein kinase A

PKB

protein kinase B

PKC

protein kinase C

PTEN

phosphatase and tensin homolog

Nanobody

A genetically encodable fragment derived from heavy chain-only antibodies found in *Camelidae* (e.g., camels, llamas, alpacas) and *Chondrichthyes* (e.g., sharks)

Molecular switch

A protein domain that can dynamically interconvert between two conformational states in response to a specific input

Photochromism

Ability of an FP to stochastically and reversibly switch between fluorescent (bright) and nonfluorescent (dark) states under specific illumination conditions

β-can

The 11-stranded β -barrel structure that surrounds the chromophore in GFP and related fluorescent proteins

Circular permutation

Shifting the positions of the native N- and C-termini along a protein's surface without altering its overall structure and function

Quantum yield

The number of photons emitted by a fluorophore per photon absorbed

Extinction coefficient

The efficiency with which a chromophore absorbs light at a specific wavelength

Literature Cited

1. Kholodenko BN, Hancock JF, Kolch W. 2010. Signalling ballet in space and time. *Nat Rev Mol Cell Biol.* 11(6):414–26 [PubMed: 20495582]
2. Brunton LL, Hayes JS, Mayer SE. 1979. Hormonally specific phosphorylation of cardiac troponin I and activation of glycogen phosphorylase. *Nature.* 280(5717):78–80 [PubMed: 15305586]
3. Steinberg SF, Brunton LL. 2001. Compartmentation of G protein-coupled signaling pathways in cardiac myocytes. *Annu. Rev. Pharmacol. Toxicol.* 41(1):751–73 [PubMed: 11264475]
4. Sample V, Mehta S, Zhang J. 2014. Genetically encoded molecular probes to visualize and perturb signaling dynamics in living biological systems. *J Cell Sci.* 127(Pt 6):1151–60 [PubMed: 24634506]
5. Zhang J 2009. The colorful journey of green fluorescent protein., Vol. 4. 4 p.
6. Rodriguez EA, Campbell RE, Lin JY, Lin MZ, Miyawaki A, et al. 2017. The Growing and Glowing Toolbox of Fluorescent and Photoactive Proteins. *Trends Biochem Sci.* 42(2):111–29 [PubMed: 27814948]
7. Greenwald EC, Mehta S, Zhang J. 2018. Genetically Encoded Fluorescent Biosensors Illuminate the Spatiotemporal Regulation of Signaling Networks. *Chem Rev.* 118(24):11707–94 [PubMed: 30550275]
8. Martin TF. 1998. Phosphoinositide lipids as signaling molecules: common themes for signal transduction, cytoskeletal regulation, and membrane trafficking. *Annu Rev Cell Dev Biol.* 14(1):231–64 [PubMed: 9891784]
9. Lemmon MA. 2003. Phosphoinositide recognition domains. *Traffic.* 4(4):201–13 [PubMed: 12694559]
10. Hurley JH, Meyer T. 2001. Subcellular targeting by membrane lipids. *Curr Opin Cell Biol.* 13(2):146–52 [PubMed: 11248547]
11. Várnai P, Balla T. 1998. Visualization of phosphoinositides that bind pleckstrin homology domains: calcium- and agonist-induced dynamic changes and relationship to myo-[3H]inositol-labeled phosphoinositide pools. *J Cell Biol.* 143(2):501–10 [PubMed: 9786958]
12. Gray A, Van Der Kaay J, Downes CP. 1999. The pleckstrin homology domains of protein kinase B and GRP1 (general receptor for phosphoinositides-1) are sensitive and selective probes for the cellular detection of phosphatidylinositol 3,4-bisphosphate and/or phosphatidylinositol 3,4,5-trisphosphate in vivo. *Biochem J.* 344 Pt 3:929–36 [PubMed: 10585883]
13. Beghein E, Gettemans J. 2017. Nanobody Technology: A Versatile Toolkit for Microscopic Imaging, Protein-Protein Interaction Analysis, and Protein Function Exploration. *Front. Immunol.* 8:771 [PubMed: 28725224]
14. Traenkle B, Emele F, Anton R, Poetz O, Haeussler RS, et al. 2015. Monitoring interactions and dynamics of endogenous beta-catenin with intracellular nanobodies in living cells. *Mol Cell Proteomics.* 14(3):707–23 [PubMed: 25595278]
15. Panza P, Maier J, Schmees C, Rothbauer U, Söllner C. 2015. Live imaging of endogenous protein dynamics in zebrafish using chromobodies. *Development.* 142(10):1879–84 [PubMed: 25968318]

16. Buchfellner A, Yurlova L, Nüske S, Scholz AM, Bogner J, et al. 2016. A New Nanobody-Based Biosensor to Study Endogenous PARP1 In Vitro and in Live Human Cells. *PLoS ONE*. 11(3):e0151041 [PubMed: 26950694]
17. Irannejad R, Tomshine JC, Tomshine JR, Chevalier M, Mahoney JP, et al. 2013. Conformational biosensors reveal GPCR signalling from endosomes. *Nature*. 495(7442):534–38 [PubMed: 23515162]
18. Ismail S, Gherardi M-J, Froese A, Zanoun M, Gigoux V, et al. 2016. Internalized Receptor for Glucose-dependent Insulinotropic Peptide stimulates adenylyl cyclase on early endosomes. *Biochemical Pharmacology*. 120:33–45 [PubMed: 27641811]
19. Regot S, Hughey JJ, Bajar BT, Carrasco S, Covert MW. 2014. High-sensitivity measurements of multiple kinase activities in live single cells. *Cell*. 157(7):1724–34 [PubMed: 24949979]
20. Kudo T, Jekni S, Macklin DN, Akhter S, Hughey JJ, et al. 2018. Live-cell measurements of kinase activity in single cells using translocation reporters. *Nat Protoc*. 13(1):155–69 [PubMed: 29266096]
21. Baird GS, Zacharias DA, Tsien RY. 1999. Circular permutation and receptor insertion within green fluorescent proteins. *Proc Natl Acad Sci USA*. 96(20):11241–46 [PubMed: 10500161]
22. Nagai T, Sawano A, Park ES, Miyawaki A. 2001. Circularly permuted green fluorescent proteins engineered to sense Ca²⁺. *Proc Natl Acad Sci USA*. 98(6):3197–3202 [PubMed: 11248055]
23. Nakai J, Ohkura M, Imoto K. 2001. A high signal-to-noise Ca(2+) probe composed of a single green fluorescent protein. *Nat Biotechnol*. 19(2):137–41 [PubMed: 11175727]
24. Barnett L, Platasa J, Popovic M, Pieribone VA, Hughes T. 2012. A fluorescent, genetically-encoded voltage probe capable of resolving action potentials. *PLoS ONE*. 7(9):e43454 [PubMed: 22970127]
25. Villette V, Chavarha M, Dimov IK, Bradley J, Pradhan L, et al. 2019. Ultrafast Two-Photon Imaging of a High-Gain Voltage Indicator in Awake Behaving Mice. *Cell*. 179(7):1590–1608.e23 [PubMed: 31835034]
26. Abdelfattah AS, Farhi SL, Zhao Y, Brinks D, Zou P, et al. 2016. A Bright and Fast Red Fluorescent Protein Voltage Indicator That Reports Neuronal Activity in Organotypic Brain Slices. *Journal of Neuroscience*. 36(8):2458–72 [PubMed: 26911693]
27. Odaka H, Arai S, Inoue T, Kitaguchi T. 2014. Genetically-encoded yellow fluorescent cAMP indicator with an expanded dynamic range for dual-color imaging. *PLoS ONE*. 9(6):e100252 [PubMed: 24959857]
28. Tewson PH, Martinka S, Shaner NC, Hughes TE, Quinn AM. 2016. New DAG and cAMP Sensors Optimized for Live-Cell Assays in Automated Laboratories. *J Biomol Screen*. 21(3):298–305 [PubMed: 26657040]
29. Hackley CR, Mazzoni EO, Blau J. 2018. CAMPr: A single-wavelength fluorescent sensor for cyclic AMP. *Sci Signal*. 11(520):eaah3738 [PubMed: 29511120]
30. Ohta Y, Furuta T, Nagai T, Horikawa K. 2018. Red fluorescent cAMP indicator with increased affinity and expanded dynamic range. *Sci Rep*. 8(1):1866 [PubMed: 29382930]
31. Bhargava Y, Hampden-Smith K, Chachlaki K, Wood KC, Vernon J, et al. 2013. Improved genetically-encoded, FlnG-type fluorescent biosensors for neural cGMP imaging. *Front Mol Neurosci*. 6:26 [PubMed: 24068983]
32. Matsuda S, Harada K, Ito M, Takizawa M, Wongso D, et al. 2017. Generation of a cGMP Indicator with an Expanded Dynamic Range by Optimization of Amino Acid Linkers between a Fluorescent Protein and PDE5 α . *ACS Sens*. 2(1):46–51 [PubMed: 28722423]
33. Lobas MA, Tao R, Nagai J, Kronschlager MT, Borden PM, et al. 2019. A genetically encoded single-wavelength sensor for imaging cytosolic and cell surface ATP. *Nat Commun*. 10(1):711 [PubMed: 30755613]
34. Hung YP, Albeck JG, Tantama M, Yellen G. 2011. Imaging cytosolic NADH-NAD(+) redox state with a genetically encoded fluorescent biosensor. *Cell Metabolism*. 14(4):545–54 [PubMed: 21982714]
35. Patriarchi T, Cho JR, Merten K, Howe MW, Marley A, et al. 2018. Ultrafast neuronal imaging of dopamine dynamics with designed genetically encoded sensors. *Science*. 360(6396):eaat4422 [PubMed: 29853555]

36. Sun F, Zeng J, Jing M, Zhou J, Feng J, et al. 2018. A Genetically Encoded Fluorescent Sensor Enables Rapid and Specific Detection of Dopamine in Flies, Fish, and Mice. *Cell*. 174(2):481–496.e19 [PubMed: 30007419]
37. Jing M, Zhang P, Wang G, Feng J, Mesik L, et al. 2018. A genetically encoded fluorescent acetylcholine indicator for in vitro and in vivo studies. *Nat Biotechnol*. 36(8):726–37 [PubMed: 29985477]
38. Mehta S, Zhang Y, Roth RH, Zhang J-F, Mo A, et al. 2018. Single-fluorophore biosensors for sensitive and multiplexed detection of signalling activities. *Nat Cell Biol*. 20(10):1215–25 [PubMed: 30250062]
39. Zhao Y, Araki S, Wu J, Teramoto T, Chang Y-F, et al. 2011. An expanded palette of genetically encoded Ca^{2+} indicators. *Science*. 333(6051):1888–91 [PubMed: 21903779]
40. Tao R, Zhao Y, Chu H, Wang A, Zhu J, et al. 2017. Genetically encoded fluorescent sensors reveal dynamic regulation of NADPH metabolism. *Nat Methods*. 14(7):720–28 [PubMed: 28581494]
41. Grynkiewicz G, Poenie M, Tsien RY. 1985. A new generation of Ca^{2+} indicators with greatly improved fluorescence properties. *J Biol Chem*. 260(6):3440–50 [PubMed: 3838314]
42. Jares-Erijman EA, Jovin TM. 2003. FRET imaging. *Nat Biotechnol*. 21(11):1387–95 [PubMed: 14595367]
43. Stryer L. 1978. Fluorescence energy transfer as a spectroscopic ruler. *Annu Rev Biochem*. 47(1):819–46 [PubMed: 354506]
44. Miyawaki A, Llopis J, Heim R, McCaffery JM, Adams JA, et al. 1997. Fluorescent indicators for Ca^{2+} based on green fluorescent proteins and calmodulin. *Nature*. 388(6645):882–87 [PubMed: 9278050]
45. Miyawaki A, Griesbeck O, Heim R, Tsien RY. 1999. Dynamic and quantitative Ca^{2+} measurements using improved cameleons. *Proc Natl Acad Sci USA*. 96(5):2135–40 [PubMed: 10051607]
46. van Dongen EMWM, Dekkers LM, Spijker K, Meijer EW, Klomp LWJ, Merkx M. 2006. Ratiometric fluorescent sensor proteins with subnanomolar affinity for Zn(II) based on copper chaperone domains. *J Am Chem Soc*. 128(33):10754–62 [PubMed: 16910670]
47. Park JG, Qin Y, Galati DF, Palmer AE. 2012. New sensors for quantitative measurement of mitochondrial Zn(2+). *ACS Chem Biol*. 7(10):1636–40 [PubMed: 22850482]
48. DiPilato LM, Cheng X, Zhang J. 2004. Fluorescent indicators of cAMP and Epac activation reveal differential dynamics of cAMP signaling within discrete subcellular compartments. *Proc Natl Acad Sci USA*. 101(47):16513–18 [PubMed: 15545605]
49. Nikolaev VO, Bünemann M, Hein L, Hannawacker A, Lohse MJ. 2004. Novel single chain cAMP sensors for receptor-induced signal propagation. *J Biol Chem*. 279(36):37215–18 [PubMed: 15231839]
50. Surdo NC, Berrera M, Koschinski A, Brescia M, Machado MR, et al. 2017. FRET biosensor uncovers cAMP nano-domains at β -adrenergic targets that dictate precise tuning of cardiac contractility. *Nat Commun*. 8:15031 [PubMed: 28425435]
51. Nikolaev VO, Gambaryan S, Lohse MJ. 2006. Fluorescent sensors for rapid monitoring of intracellular cGMP. *Nat Methods*. 3(1):23–25 [PubMed: 16369548]
52. Sato M, Hida N, Ozawa T, Umezawa Y. 2000. Fluorescent Indicators for Cyclic GMP Based on Cyclic GMP-Dependent Protein Kinase I α and Green Fluorescent Proteins. *Anal. Chem*. 72(24):5918–24 [PubMed: 11140757]
53. Calamera G, Li D, Ulsund AH, Kim JJ, Neely OC, et al. 2019. FRET-based cyclic GMP biosensors measure low cGMP concentrations in cardiomyocytes and neurons. *Commun Biol*. 2(1):394–12 [PubMed: 31701023]
54. Sato M, Ueda Y, Takagi T, Umezawa Y. 2003. Production of PtdInsP3 at endomembranes is triggered by receptor endocytosis. *Nat Cell Biol*. 5(11):1016–22 [PubMed: 14528311]
55. Ananthanarayanan B, Ni Q, Zhang J. 2005. Signal propagation from membrane messengers to nuclear effectors revealed by reporters of phosphoinositide dynamics and Akt activity. *Proc Natl Acad Sci USA*. 102(42):15081–86 [PubMed: 16214892]
56. Hertel F, Li S, Chen M, Pott L, Mehta S, Zhang J. 2020. Fluorescent Biosensors for Multiplexed Imaging of Phosphoinositide Dynamics. *ACS Chem Biol*. 15(1):33–38 [PubMed: 31855412]

57. Zhang J, Hupfeld CJ, Taylor SS, Olefsky JM, Tsien RY. 2005. Insulin disrupts beta-adrenergic signalling to protein kinase A in adipocytes. *Nature*. 437(7058):569–73 [PubMed: 16177793]
58. Ma L, Jongbloets BC, Xiong W-H, Melander JB, Qin M, et al. 2018. A Highly Sensitive A-Kinase Activity Reporter for Imaging Neuromodulatory Events in Awake Mice. *Neuron*. 99(4):665–65 [PubMed: 30100256]
59. Violin JD, Zhang J, Tsien RY, Newton AC. 2003. A genetically encoded fluorescent reporter reveals oscillatory phosphorylation by protein kinase C. *J Cell Biol*. 161(5):899–909 [PubMed: 12782683]
60. Ross BL, Tenner B, Markwardt ML, Zviman A, Shi G, et al. 2018. Single-color, ratiometric biosensors for detecting signaling activities in live cells. *Elife*. 7:e35458 [PubMed: 29968564]
61. Kunkel MT, Kunkel MT, Ni Q, Tsien RY, Zhang J, Newton AC. 2005. Spatio-temporal dynamics of protein kinase B/Akt signaling revealed by a genetically encoded fluorescent reporter. *J Biol Chem*. 280(7):5581–87 [PubMed: 15583002]
62. Harvey CD, Ehrhardt AG, Cellurale C, Zhong H, Yasuda R, et al. 2008. A genetically encoded fluorescent sensor of ERK activity. *Proc Natl Acad Sci USA*. 105(49):19264–69 [PubMed: 19033456]
63. Fuller BG, Lampson MA, Foley EA, Rosasco-Nitcher S, Le KV, et al. 2008. Midzone activation of aurora B in anaphase produces an intracellular phosphorylation gradient. *Nature*. 453(7198):1132–36 [PubMed: 18463638]
64. Mochizuki N, Yamashita S, Kurokawa K, Ohba Y, Nagai T, et al. 2001. Spatio-temporal images of growth-factor-induced activation of Ras and Rap1. *Nature*. 411(6841):1065–68 [PubMed: 11429608]
65. Kitano M, Nakaya M, Nakamura T, Nagata S, Matsuda M. 2008. Imaging of Rab5 activity identifies essential regulators for phagosome maturation. *Nature*. 453(7192):241–45 [PubMed: 18385674]
66. Zawistowski JS, Sabouri-Ghomi M, Danuser G, Hahn KM, Hodgson L. 2013. A RhoC biosensor reveals differences in the activation kinetics of RhoA and RhoC in migrating cells. *PLoS ONE*. 8(11):e79877 [PubMed: 24224016]
67. Bastiaens PI, Squire A. 1999. Fluorescence lifetime imaging microscopy: spatial resolution of biochemical processes in the cell. *Trends Cell Biol*. 9(2):48–52 [PubMed: 10087617]
68. Calebiro D, Nikolaev VO, Gagliani MC, de Filippis T, Dees C, et al. 2009. Persistent cAMP-signals triggered by internalized G-protein-coupled receptors. *PLoS Biol*. 7(8):e1000172 [PubMed: 19688034]
69. Ferrandon S, Feinstein TN, Castro M, Wang B, Bouley R, et al. 2009. Sustained cyclic AMP production by parathyroid hormone receptor endocytosis. *Nat Chem Biol*. 5(10):734–42 [PubMed: 19701185]
70. Godbole A, Lyga S, Lohse MJ, Calebiro D. 2017. Internalized TSH receptors en route to the TGN induce local Gs-protein signaling and gene transcription. *Nat Commun*. 8(1):443 [PubMed: 28874659]
71. Irannejad R, Pessino V, Mika D, Huang B, Wedegaertner PB, et al. 2017. Functional selectivity of GPCR-directed drug action through location bias. *Nat Chem Biol*. 13(7):799–806 [PubMed: 28553949]
72. Nash CA, Wei W, Irannejad R, Smrcka AV. 2019. Golgi localized β 1-adrenergic receptors stimulate Golgi PI4P hydrolysis by PLC ϵ to regulate cardiac hypertrophy. *Elife*. 8:10140
73. Eichel K, Zastrow von M. 2018. Subcellular Organization of GPCR Signaling. *Trends Pharmacol Sci*. 39(2):200–208 [PubMed: 29478570]
74. Allen MD, Zhang J. 2006. Subcellular dynamics of protein kinase A activity visualized by FRET-based reporters. *Biochem Biophys Res Commun*. 348(2):716–21 [PubMed: 16895723]
75. Gallegos LL, Kunkel MT, Newton AC. 2006. Targeting protein kinase C activity reporter to discrete intracellular regions reveals spatiotemporal differences in agonist-dependent signaling. *J Biol Chem*. 281(41):30947–56 [PubMed: 16901905]
76. Kunkel MT, Toker A, Tsien RY, Newton AC. 2007. Calcium-dependent regulation of protein kinase D revealed by a genetically encoded kinase activity reporter. *J Biol Chem*. 282(9):6733–42 [PubMed: 17189263]

77. Mehta S, Aye-Han N-N, Ganesan A, Oldach L, Gorshkov K, Zhang J. 2014. Calmodulin-controlled spatial decoding of oscillatory Ca²⁺ signals by calcineurin. *Elife*. 3:e03765 [PubMed: 25056880]
78. Zhou X, Clister TL, Lowry PR, Seldin MM, Wong GW, Zhang J. 2015. Dynamic Visualization of mTORC1 Activity in Living Cells. *Cell Rep*. 10(10):1767–77 [PubMed: 25772363]
79. Kim J, Guan K-L. 2019. mTOR as a central hub of nutrient signalling and cell growth. *Nat Cell Biol*. 21(1):63–71 [PubMed: 30602761]
80. Wu H, Carvalho P, Voeltz GK. 2018. Here, there, and everywhere: The importance of ER membrane contact sites. *Science*. 361(6401):eaan5835 [PubMed: 30072511]
81. Scorrano L, De Matteis MA, Emr S, Giordano F, Hajnóczky G, et al. 2019. Coming together to define membrane contact sites. *Nat Commun*. 10(1):1287–11 [PubMed: 30894536]
82. BERNHARD W, ROUILLER C 1956. Close topographical relationship between mitochondria and ergastoplasm of liver cells in a definite phase of cellular activity. *J Biophys Biochem Cytol*. 2(4 Suppl):73–78 [PubMed: 13357525]
83. COPELAND DE, DALTON AJ. 1959. An association between mitochondria and the endoplasmic reticulum in cells of the pseudobranch gland of a teleost. *J Biophys Biochem Cytol*. 5(3):393–96 [PubMed: 13664679]
84. Jones PP, MacQuaide N, Louch WE. 2018. Dyadic Plasticity in Cardiomyocytes. *Front Physiol*. 9:1773 [PubMed: 30618792]
85. Chen T-W, Wardill TJ, Sun Y, Pulver SR, Renninger SL, et al. 2013. Ultrasensitive fluorescent proteins for imaging neuronal activity. *Nature*. 499(7458):295–300 [PubMed: 23868258]
86. Shang W, Lu F, Sun T, Xu J, Li L-L, et al. 2014. Imaging Ca²⁺ nanosparks in heart with a new targeted biosensor. *Circ Res*. 114(3):412–20 [PubMed: 24257462]
87. Lee MY, Song H, Nakai J, Ohkura M, Kotlikoff MI, et al. 2006. Local subplasma membrane Ca²⁺ signals detected by a tethered Ca²⁺ sensor. *Proc Natl Acad Sci USA*. 103(35):13232–37 [PubMed: 16924099]
88. Chang C-L, Chen Y-J, Liou J. 2017. ER-plasma membrane junctions: Why and how do we study them? *BBA - Molecular Cell Research*. 1864(9):1494–1506 [PubMed: 28554772]
89. Song H, Lee MY, Kinsey SP, Weber DJ, Blaustein MP. 2006. An N-terminal sequence targets and tethers Na⁺ pump alpha2 subunits to specialized plasma membrane microdomains. *J Biol Chem*. 281(18):12929–40 [PubMed: 16524882]
90. Agarwal A, Wu P-H, Hughes EG, Fukaya M, Tischfield MA, et al. 2017. Transient Opening of the Mitochondrial Permeability Transition Pore Induces Microdomain Calcium Transients in Astrocyte Processes. *Neuron*. 93(3):587–87 [PubMed: 28132831]
91. Tian L, Hires SA, Mao T, Huber D, Chiappe ME, et al. 2009. Imaging neural activity in worms, flies and mice with improved GCaMP calcium indicators. *Nat Methods*. 6(12):875–81 [PubMed: 19898485]
92. Bernardi P, Petronilli V. 1996. The permeability transition pore as a mitochondrial calcium release channel: a critical appraisal. *J Bioenerg Biomembr*. 28(2):131–38 [PubMed: 9132411]
93. Kuchibhotla KV, Lattarulo CR, Hyman BT, Bacskai BJ. 2009. Synchronous hyperactivity and intercellular calcium waves in astrocytes in Alzheimer mice. *Science*. 323(5918):1211–15 [PubMed: 19251629]
94. Simons K, Simons K, Toomre D. 2000. Lipid rafts and signal transduction. *Nat Rev Mol Cell Biol*. 1(1):31–39 [PubMed: 11413487]
95. Sezgin E, Levental I, Mayor S, Eggeling C. 2017. The mystery of membrane organization: composition, regulation and roles of lipid rafts. *Nat Rev Mol Cell Biol*. 18(6):361–74 [PubMed: 28356571]
96. Zacharias DA, Violin JD, Newton AC, Tsien RY. 2002. Partitioning of lipid-modified monomeric GFPs into membrane microdomains of live cells. *Science*. 296(5569):913–16 [PubMed: 11988576]
97. Lasserre R, Guo X-J, Conchonaud F, Hamon Y, Hawchar O, et al. 2008. Raft nanodomains contribute to Akt/PKB plasma membrane recruitment and activation. *Nat Chem Biol*. 4(9):538–47 [PubMed: 18641634]
98. Gao X, Zhang J. 2008. Spatiotemporal analysis of differential Akt regulation in plasma membrane microdomains. *Mol Biol Cell*. 19(10):4366–73 [PubMed: 18701703]

99. Gao X, Lowry PR, Zhou X, Depry C, Wei Z, et al. 2011. PI3K/Akt signaling requires spatial compartmentalization in plasma membrane microdomains. *Proc Natl Acad Sci USA*. 108(35):14509–14 [PubMed: 21873248]
100. Seong J, Huang M, Sim KM, Kim H, Wang Y. 2017. FRET-based Visualization of PDGF Receptor Activation at Membrane Microdomains. *Sci Rep*. 7(1):1593 [PubMed: 28487538]
101. Wu H 2013. Higher-order assemblies in a new paradigm of signal transduction. *Cell*. 153(2):287–92 [PubMed: 23582320]
102. Lillemeier BF, Mörtelmaier MA, Forstner MB, Huppa JB, Groves JT, Davis MM. 2010. TCR and Lat are expressed on separate protein islands on T cell membranes and concatenate during activation. *Nat. Immunol*. 11(1):90–96 [PubMed: 20010844]
103. Ma Y, Pandzic E, Nicovich PR, Yamamoto Y, Kwiatek J, et al. 2017. An intermolecular FRET sensor detects the dynamics of T cell receptor clustering. *Nat Commun*. 8:15100 [PubMed: 28452360]
104. Wachten S, Masada N, Ayling L-J, Ciruela A, Nikolaev VO, et al. 2010. Distinct pools of cAMP centre on different isoforms of adenylyl cyclase in pituitary-derived GH3B6 cells. *J Cell Sci*. 123(Pt 1):95–106 [PubMed: 20016070]
105. Tallini YN, Ohkura M, Choi B-R, Ji G, Imoto K, et al. 2006. Imaging cellular signals in the heart in vivo: Cardiac expression of the high-signal Ca²⁺ indicator GCaMP2. *Proc Natl Acad Sci USA*. 103(12):4753–58 [PubMed: 16537386]
106. Willoughby D, Wachten S, Masada N, Cooper DMF. 2010. Direct demonstration of discrete Ca²⁺ microdomains associated with different isoforms of adenylyl cyclase. *J Cell Sci*. 123(Pt 1):107–17 [PubMed: 20016071]
107. Lohse C, Bock A, Maiellaro I, Hannawacker A, Schad LR, et al. 2017. Experimental and mathematical analysis of cAMP nanodomains. *PLoS ONE*. 12(4):e0174856 [PubMed: 28406920]
108. Zaccolo M, Di Benedetto G, Lissandron V, Mancuso L, Terrin A, Zamparo I. 2006. Restricted diffusion of a freely diffusible second messenger: mechanisms underlying compartmentalized cAMP signalling. *Biochem Soc Trans*. 34(Pt 4):495–97 [PubMed: 16856842]
109. Baillie GS. 2009. Compartmentalized signalling: spatial regulation of cAMP by the action of compartmentalized phosphodiesterases. *FEBS J*. 276(7):1790–99 [PubMed: 19243430]
110. Clister T, Greenwald EC, Baillie GS, Zhang J. 2019. AKAP95 Organizes a Nuclear Microdomain to Control Local cAMP for Regulating Nuclear PKA. *Cell Chem Biol*. 26(6):885–891.e4 [PubMed: 30982750]
111. DiPilato LM, Zhang J. 2009. The role of membrane microdomains in shaping beta2-adrenergic receptor-mediated cAMP dynamics. *Mol Biosyst*. 5(8):832–37 [PubMed: 19603118]
112. Sample V, DiPilato LM, Yang JH, Ni Q, Saucerman JJ, Zhang J. 2012. Regulation of nuclear PKA revealed by spatiotemporal manipulation of cyclic AMP. *Nat Chem Biol*. 8(4):375–82 [PubMed: 22366721]
113. Haugh JM, Codazzi F, Teruel M, Meyer T. 2000. Spatial sensing in fibroblasts mediated by 3' phosphoinositides. *J Cell Biol*. 151(6):1269–80 [PubMed: 11121441]
114. Servant G, Weiner OD, Herzmark P, Balla T, Sedat JW, Bourne HR. 2000. Polarization of chemoattractant receptor signaling during neutrophil chemotaxis. *Science*. 287(5455):1037–40 [PubMed: 10669415]
115. Funamoto S, Meili R, Lee S, Parry L, Firtel RA. 2002. Spatial and temporal regulation of 3-phosphoinositides by PI 3-kinase and PTEN mediates chemotaxis. *Cell*. 109(5):611–23 [PubMed: 12062104]
116. Kim JM, Lee M, Kim N, Heo WD. 2016. Optogenetic toolkit reveals the role of Ca²⁺ sparklets in coordinated cell migration. *Proc Natl Acad Sci USA*. 113(21):5952–57 [PubMed: 27190091]
117. Gorshkov K, Mehta S, Ramamurthy S, Ronnett GV, Zhou F-Q, Zhang J. 2017. AKAP-mediated feedback control of cAMP gradients in developing hippocampal neurons. *Nat Chem Biol*. 13(4):425–31 [PubMed: 28192412]
118. Maiellaro I, Lohse MJ, Kittel RJ, Calebiro D. 2016. cAMP Signals in Drosophila Motor Neurons Are Confined to Single Synaptic Boutons. *Cell Rep*. 17(5):1238–46 [PubMed: 27783939]

119. Cugno A, Bartol TM, Sejnowski TJ, Iyengar R, Rangamani P. 2019. Geometric principles of second messenger dynamics in dendritic spines. *Sci Rep.* 9(1):11676–18 [PubMed: 31406140]
120. Neves SR, Tsokas P, Sarkar A, Grace EA, Rangamani P, et al. 2008. Cell shape and negative links in regulatory motifs together control spatial information flow in signaling networks. *Cell.* 133(4):666–80 [PubMed: 18485874]
121. Milo R, Jorgensen P, Moran U, Weber G, Springer M. 2010. BioNumbers--the database of key numbers in molecular and cell biology. *Nucleic Acids Res.* 38(Database issue):D750–53 [PubMed: 19854939]
122. An S, Kumar R, Sheets ED, Benkovic SJ. 2008. Reversible compartmentalization of de novo purine biosynthetic complexes in living cells. *Science.* 320(5872):103–6 [PubMed: 18388293]
123. Kohnhorst CL, Kyoung M, Jeon M, Schmitt DL, Kennedy EL, et al. 2017. Identification of a Multienzyme Complex for Glucose Metabolism in Living Cells. *J Biol Chem.* 292(22):9191–9203 [PubMed: 28424264]
124. Greenwald EC, Saucerman JJ. 2011. Bigger, better, faster: principles and models of AKAP anchoring protein signaling. *J. Cardiovasc. Pharmacol.* 58(5):462–69 [PubMed: 21562426]
125. Good MC, Zalatan JG, Lim WA. 2011. Scaffold proteins: hubs for controlling the flow of cellular information. *Science.* 332(6030):680–86 [PubMed: 21551057]
126. Wong W, Scott JD. 2004. AKAP signalling complexes: focal points in space and time. *Nat Rev Mol Cell Biol.* 5(12):959–70 [PubMed: 15573134]
127. Dodge-Kafka KL, Souhayer J, Pare GC, Carlisle Michel JJ, Langeberg LK, et al. 2005. The protein kinase A anchoring protein mAKAP coordinates two integrated cAMP effector pathways. *Nature.* 437(7058):574–78 [PubMed: 16177794]
128. Kapiloff MS, Piggott LA, Sadana R, Li J, Heredia LA, et al. 2009. An adenylyl cyclase-mAKAPbeta signaling complex regulates cAMP levels in cardiac myocytes. *J Biol Chem.* 284(35):23540–46 [PubMed: 19574217]
129. Boczek T, Cameron EG, Yu W, Xia X, Shah SH, et al. 2019. Regulation of Neuronal Survival and Axon Growth by a Perinuclear cAMP Compartment. *Journal of Neuroscience.* 39(28):5466–80 [PubMed: 31097623]
130. Tobias IS, Newton AC. 2016. Protein Scaffolds Control Localized Protein Kinase C ζ Activity. *J Biol Chem.* 291(26):13809–22 [PubMed: 27143478]
131. Brown MD, Sacks DB. 2009. Protein scaffolds in MAP kinase signalling. *Cell Signal.* 21(4):462–69 [PubMed: 19091303]
132. Jang ER, Galperin E. 2016. The function of Shoc2: A scaffold and beyond. *Commun Integr Biol.* 9(4):e1188241 [PubMed: 27574535]
133. Terai K, Matsuda M. 2005. Ras binding opens c-Raf to expose the docking site for mitogen-activated protein kinase kinase. *EMBO Rep.* 6(3):251–55 [PubMed: 15711535]
134. Yoshiki S, Matsunaga-Udagawa R, Aoki K, Kamioka Y, Kiyokawa E, Matsuda M. 2010. Ras and calcium signaling pathways converge at Raf1 via the Shoc2 scaffold protein. *Mol Biol Cell.* 21(6):1088–96 [PubMed: 20071468]
135. Matsunaga-Udagawa R, Fujita Y, Yoshiki S, Terai K, Kamioka Y, et al. 2010. The scaffold protein Shoc2/SUR-8 accelerates the interaction of Ras and Raf. *J Biol Chem.* 285(10):7818–26 [PubMed: 20051520]
136. Mo GCH, Ross B, Hertel F, Manna P, Yang X, et al. 2017. Genetically encoded biosensors for visualizing live-cell biochemical activity at super-resolution. *Nat Methods.* 14(4):427–34 [PubMed: 28288122]
137. Dedecker P, Mo GCH, Dertinger T, Zhang J. 2012. Widely accessible method for superresolution fluorescence imaging of living systems. *Proc Natl Acad Sci USA.* 109(27):10909–14 [PubMed: 22711840]
138. Nobis M, McGhee EJ, Morton JP, Schwarz JP, Karim SA, et al. 2013. Intravital FLIM-FRET imaging reveals dasatinib-induced spatial control of src in pancreatic cancer. *Cancer Res.* 73(15):4674–86 [PubMed: 23749641]
139. Mizutani T, Kondo T, Darmanin S, Tsuda M, Tanaka S, et al. 2010. A novel FRET-based biosensor for the measurement of BCR-ABL activity and its response to drugs in living cells. *Clin. Cancer Res.* 16(15):3964–75 [PubMed: 20670950]

140. Kondo T, Fujioka M, Tsuda M, Murai K, Yamaguchi K, et al. 2018. Pretreatment evaluation of fluorescence resonance energy transfer-based drug sensitivity test for patients with chronic myelogenous leukemia treated with dasatinib. *Cancer Sci.* 109(7):2256–65 [PubMed: 29719934]
141. Kondo T, Fujioka M, Fujisawa S, Sato K, Tsuda M, et al. 2019. Clinical efficacy and safety of first-line nilotinib therapy and evaluation of the clinical utility of the FRET-based drug sensitivity test. *Int. J. Hematol.* 110(4):482–89 [PubMed: 31240558]
142. Zhao Y, Hu Q, Cheng F, Su N, Wang A, et al. 2015. SoNar, a Highly Responsive NAD⁺/NADH Sensor, Allows High-Throughput Metabolic Screening of Anti-tumor Agents. *Cell Metabolism.* 21(5):777–89 [PubMed: 25955212]
143. San Martín A, Ceballo S, Ruminot I, Lerchundi R, Frommer WB, Barros LF. 2013. A genetically encoded FRET lactate sensor and its use to detect the Warburg effect in single cancer cells. *PLoS ONE.* 8(2):e57712 [PubMed: 23469056]
144. Contreras-Baeza Y, Ceballo S, Arce-Molina R, Sandoval PY, Alegría K, et al. 2019. MitoToxy assay: A novel cell-based method for the assessment of metabolic toxicity in a multiwell plate format using a lactate FRET nanosensor, Laconic. *PLoS ONE.* 14(10):e0224527 [PubMed: 31671132]
145. Helmchen F, Denk W. 2005. Deep tissue two-photon microscopy. *Nat Methods.* 2(12):932–40 [PubMed: 16299478]
146. To T-L, Piggott BJ, Makhijani K, Yu D, Jan YN, Shu X. 2015. Rationally designed fluorogenic protease reporter visualizes spatiotemporal dynamics of apoptosis in vivo. *Proc Natl Acad Sci USA.* 112(11):3338–43 [PubMed: 25733847]
147. Qian Y, Piatkevich KD, Mc Larney B, Abdelfattah AS, Mehta S, et al. 2019. A genetically encoded near-infrared fluorescent calcium ion indicator. *Nat Methods.* 16(2):171–74 [PubMed: 30664778]
148. Shcherbakova DM, Cox Cammer N, Huisman TM, Verkhusha VV, Hodgson L. 2018. Direct multiplex imaging and optogenetics of Rho GTPases enabled by near-infrared FRET. *Nat Chem Biol.* 14(6):591–600 [PubMed: 29686359]
149. Hyman AA, Weber CA, Jülicher F. 2014. Liquid-liquid phase separation in biology. *Annu Rev Cell Dev Biol.* 30:39–58 [PubMed: 25288112]
150. Banani SF, Lee HO, Hyman AA, Rosen MK. 2017. Biomolecular condensates: organizers of cellular biochemistry. *Nat Rev Mol Cell Biol.* 18(5):285–98 [PubMed: 28225081]
151. Wright PE, Dyson HJ. 2015. Intrinsically disordered proteins in cellular signalling and regulation. *Nat Rev Mol Cell Biol.* 16(1):18–29 [PubMed: 25531225]
152. Chong PA, Forman-Kay JD. 2016. Liquid-liquid phase separation in cellular signaling systems. *Curr Opin Struct Biol.* 41:180–86 [PubMed: 27552079]

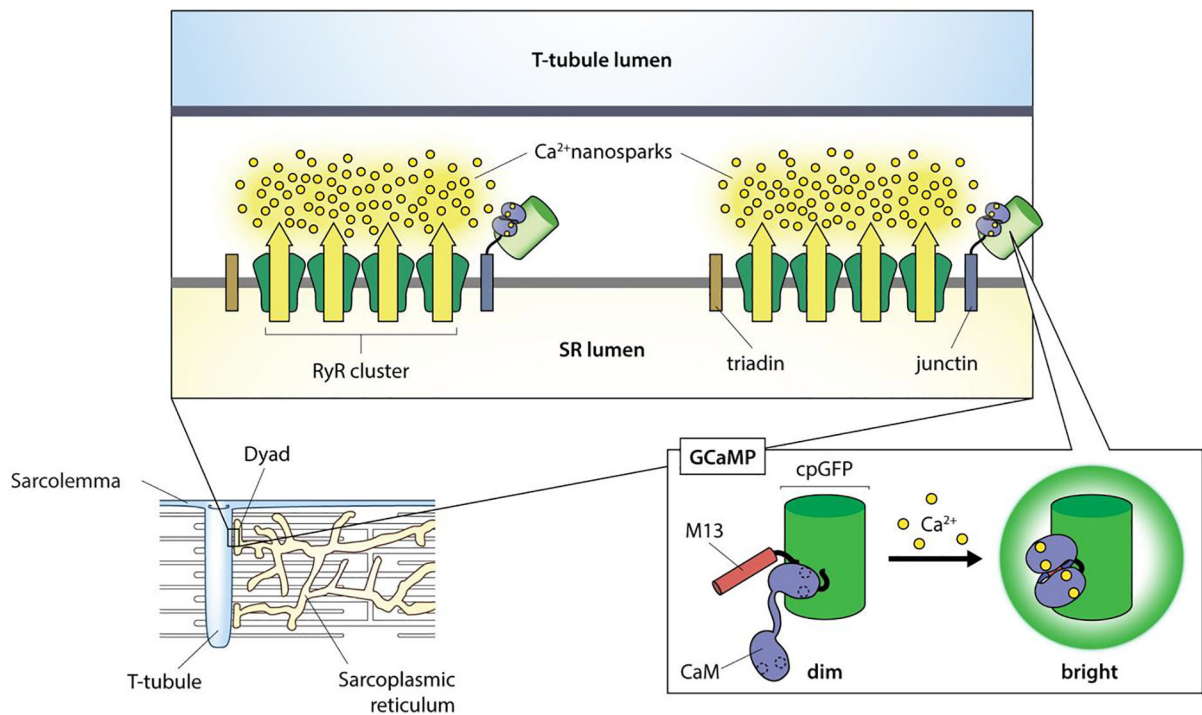


Figure 1. A Ca^{2+} microdomain formed by opposing membranes in cardiomyocytes.

Close apposition of the sarcoplasmic reticulum (SR) and sarcolemma along T-tubules in cardiomyocytes forms unique signaling microdomains known as dyads. These membrane contact sites are characterized by clusters of ryanodine receptors (RyRs) on the SR surface, which release Ca^{2+} into the dyadic cleft. To selectively monitor Ca^{2+} signaling within this microdomain, Shang et al. (86) tethered the Ca^{2+} sensor GCaMP to either junctin or triadin, which localize to the SR membrane in dyads. This approach allowed the authors to detect and visualize discrete Ca^{2+} “nanosparks” originating from the spontaneous firing of individual RyR clusters. Inset: GCaMP consists of circularly permuted GFP (cpGFP) sandwiched between the Ca^{2+} -binding protein calmodulin (CaM) and the CaM-binding M13 peptide. Upon Ca^{2+} binding, CaM forms a complex with the M13 peptide, leading to a conformational change that increases the brightness of GFP.

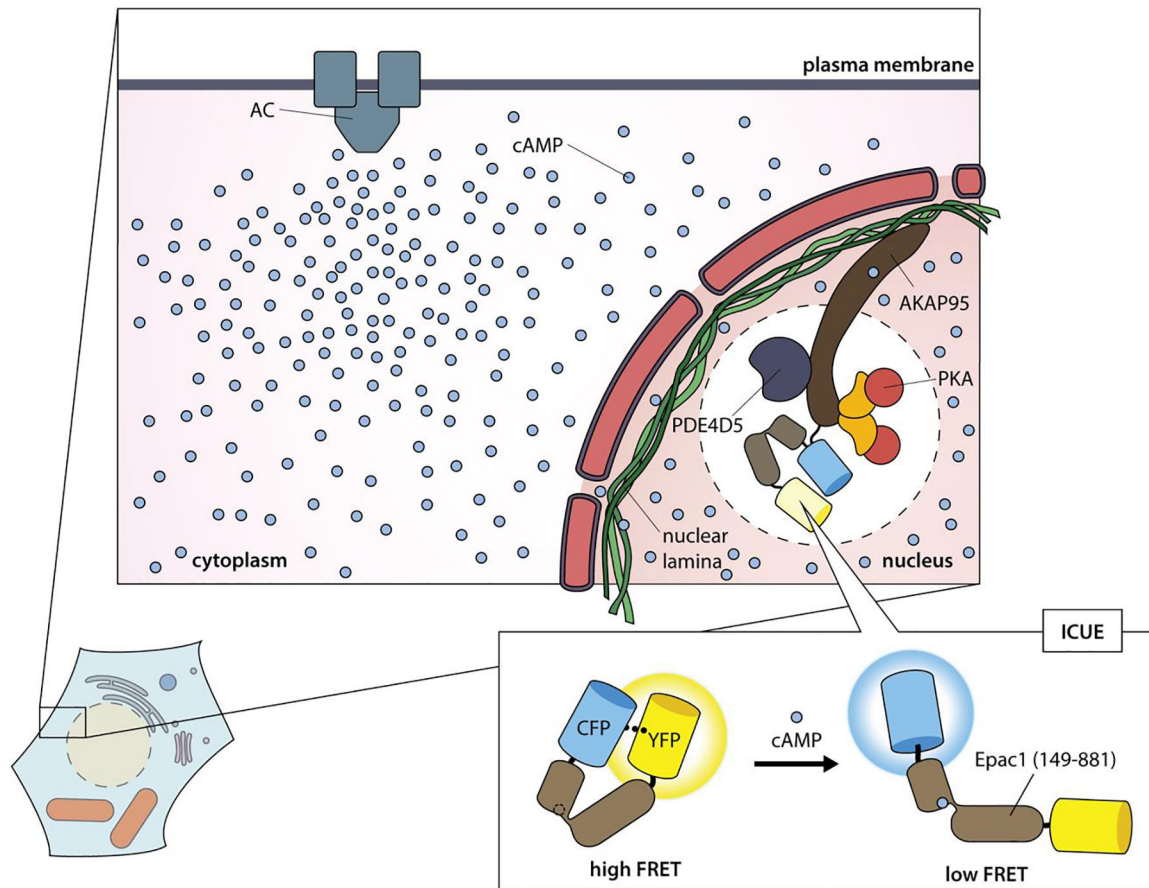


Figure 2. PDE activity fences off a sub-nuclear cAMP microdomain.

Phosphodiesterases (PDEs) catalyze the degradation of cAMP and play a major role in compartmentalizing cAMP signaling. By limiting cAMP diffusion, PDEs can act as fences that prevent cAMP from exiting a particular microdomain. However, local cAMP degradation by anchored PDEs can alternatively act as a fence to exclude cAMP from entering a microdomain. This was recently illustrated by Clister et al. (108), who were able to observe the formation of a discrete sub-nuclear signaling microdomain when they tethered the FRET-based cAMP sensor ICUE to the nuclear-localized scaffold AKAP95. This tethered sensor was unable to detect cAMP elevations originating from the plasma membrane due to the activity of AKAP95-bound PDE4D5, revealing the formation of a signaling microdomain that is specifically insulated from plasma membrane cAMP signaling. Inset: ICUE contains a fragment of the cAMP-binding protein Epac1 sandwiched between CFP and YFP. cAMP binding switches Epac1 from a compact, closed conformation to an open, extended conformation that results in a decrease in FRET between CFP and YFP.

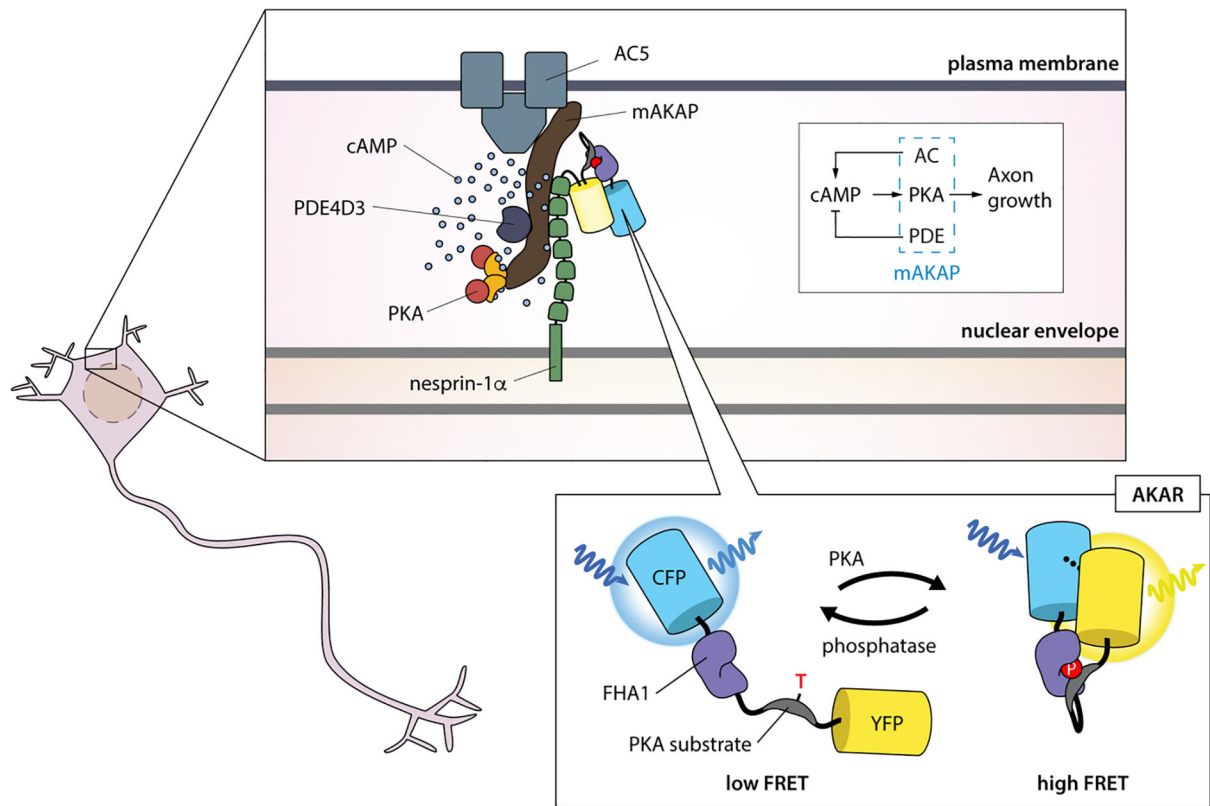


Figure 3. Formation of a perinuclear signaling circuit via molecular assembly.

cAMP signaling is a key regulator of multiple processes during nervous system development, including axon growth in neurons. AKAPs help compartmentalize cAMP signaling by facilitating the assembly of molecular complexes in which the machinery needed to produce (AC), degrade (PDE), and transduce (PKA) cAMP signals form self-contained local circuits. Boczek et al. (126) studied one such microdomain formed by mAKAP, which assembles AC5, PDE4D3, and PKA into a perinuclear microdomain. By tethering the FRET-based PKA activity reporter AKAR to nesprin-1 α , which localizes mAKAP to the nuclear envelope, they were able to visualize the regulation of PKA signaling within the mAKAP microdomain and discover that local signaling by this perinuclear circuit is crucial for driving axon elongation in hippocampal neurons. Inset: AKAR utilizes a molecular switch containing a PKA substrate peptide linked to the phosphoamino acid-binding FHA1 domain, which is sandwiched between CFP and YFP. Phosphorylation of the substrate peptide by PKA triggers recognition and binding by FHA1, which causes the sensor to adopt a more compact conformation that increases FRET between CFP and YFP.